

Stopped-Flow Small-Angle X-Ray Scattering Study on the Acid-Denaturation of Taka-Amylase A

Tatsuya HOZAKI,[†] Mitsunori KATO,[†] Mamoru SATO,^{*} Nobuo TANAKA, Yukio MORIMOTO, Yasuo HATA, Yukiteru KATSUBE, and Nobutami KASAI[†]

Institute for Protein Research, Osaka University

[†]Department of Applied Chemistry, Faculty of Engineering, Osaka University, Suita, Osaka 565

(Received May 21, 1986)

A stopped-flow small-angle X-ray scattering method was applied to study the structural change of Taka-amylase A by acid-denaturation. The structural change could be described by two successive steps. The first step is described by a change in the eccentricity of a prolate ellipsoid from 2.0 to 2.4; this was estimated by a comparison between the observed scattering profile and the theoretical scattering function of the prolate ellipsoid. The second step supposes that the X-ray scatterer in a solution comprises two kinds of particles with large and small radii of gyration. The X-ray scatterer with a large radius expands with time. By contrast, the radius of gyration of the small scatterer corresponds to that of a native Taka-amylase A monomer and it remains unchanged. These facts imply that in the denaturation of Taka-amylase A the molecule is prolonged by a partial unfolding of the polypeptide chain and then aggregates with each other.

Taka-amylase A (EC 3.2.1.1, α -1,4-glucan-4-glucanohydrolase) is an α -amylase that catalyzes the hydrolysis of α -1,4-glucosidic linkages in polysaccharides. Many studies have been undertaken on Taka-amylase A since Akabori and Okahara extracted the enzyme from *Aspergillus oryzae*.¹⁾ The enzyme is monomeric, composed of a single polypeptide chain (478 amino acid residues²⁾) and has a molecular weight of 51000. The three-dimensional structure of Taka-amylase A has been determined at a 3.0-Å resolution by an X-ray crystal structure analysis,³⁾ and the mechanism of its enzymatic activity has been proposed.⁴⁾

Takagi et al. have studied the renaturation of Taka-amylase A from an acid- or a urea-denaturated molecule by such means as optical rotatory dispersion, pH titration, and sedimentation velocity.^{5–7)} They have suggested that through acid-denaturation the hydrogen bonds between the side-chain groups are completely cleaved and most of the peptide hydrogen bonds are retained to maintain the structure of the helical region, though the urea-denaturation results in unfolded molecules devoid of secondary and tertiary structures. It has also been reported that the acid-denaturation of Taka-amylase A proceeds very slowly at pH 3.3 with a time resolution of 1 min.⁵⁾ For studies concerning the slow change in the structure, it is useful to analyze the structural change with a small-angle X-ray scattering method with a stopped-flow mixing device and a position-sensitive detector. From these points of view, the present paper concerns a study of the time-resolved structural change of Taka-amylase A by acid-denaturation at pH 3.3 by means of stopped-flow small-angle X-ray scattering.

Experimental

Sample Preparation for X-Ray Experiments. Taka-amylase A was isolated from Takadiastase Sankyo according to the method of Akabori et al.,⁸⁾ and purified with chromatography on a DEAE-cellulose column. The eluent from the column was desalted by ultrafiltration with a Diaflo YM-30

membrane followed by a repeated addition of distilled water. At the end of the desalting process, the purified protein solution was concentrated to more than 70 mg ml⁻¹ by ultrafiltration. The protein concentration of the purified Taka-amylase A, which was determined spectrophotometrically by UV absorption at 279 nm by using $E_{1\%}^{1\text{cm}} = 22.1$, was then adjusted to be 20.0 mg ml⁻¹ by diluting the solution with distilled water. The protein solution was mixed with a 0.1-M glycine/NaCl-HCl (1 M=1 mol dm⁻³) buffer in the stopped-flow mixing device. The pH of the buffer was determined so that the pH of the mixed solution might be 3.3 (tested at each temperature before X-ray experiments).

Stopped-Flow Mixing Device. A stopped-flow mixing device was constructed by Union Giken Co. Ltd.. Equal volumes of two solutions were mixed in a jet mixer and transferred into a 1.0-mm ϕ thin-walled quartz capillary using the pressure difference of nitrogen gas; this was also used for draining the mixed solution. The irradiated area was modified so that line-collimated X-rays could completely irradiate the capillary. The temperature in the device was controlled by circulating water with a constant temperature. The temperature of the mixed solution was detected by a copper-constantan thermocouple located beside the capillary and was monitored on a recorder. The dead time between the transmission of the signal and the filling of the tube with the mixed solution was about 100 ms. No meaningful difference was found between the scattering intensity distribution of the distilled water obtained from one time accumulation of 200-s measured data and that obtained from 2000 accumulations of 100-ms measured data. This shows that no mixing artifact was observed during the experiments. About 100 μ l of a mixed solution was consumed per shot. The capillary was washed out with two shots of immediately mixed solution just before each measurement was started. All operations for the stopped-flow mixing device were controlled with a microcomputer connected with an X-ray detector.

X-Ray Measurements. The X-ray source was a 0.4 \times 8 mm spot on the copper anode of a Philips fine-focus X-ray tube operated with a Rigaku Denki D9C X-ray generator run at 40 kV, 30 mA. A line focus was used to obtain sufficiently intense scattered X-rays. The spot was foreshortened to 0.04 \times 8 mm at a glancing angle of 6°. The nickel-filtered (10 μ m in thickness) X-rays were collimated with a 0.3 \times 10

mm slit, and then reflected and focussed by a nickel-coated glass mirror⁹) through two kinds of limiting slits. One was located immediately after a mirror holder to collimate reflected X-rays; the other was located just before a stopped-flow mixing device to reduce the parasitic scattering originating from the edge of the former slit. The scattered X-rays were recorded on a one-dimensional position-sensitive proportional detector (delay-line type). The flowing gas (11 mm in thickness) used was a mixture of 90% argon and 10% methane. The width of the detector window was 10 mm. The detector length was 50 mm and was divided into 256 channels on a multichannel analyzer. The sample-to-detector distance was 310.0 mm. The scattered X-rays were collected in the range of the scattering angles from 3.8×10^{-3} to 7.7×10^{-2} rad. The X-ray path from the stopped-flow mixing device to the detector was evacuated to avoid air scattering. All the X-ray camera units were located in the small chamber with the temperature controlled to be 5°C (with a cooling unit) in order to prevent dew from appearing on and in the stopped-flow mixing device during low-temperature experiments. X-Ray experiments were performed at 0, 5, 10, and 15°C, respectively. These temperatures were kept within $\pm 0.1^\circ\text{C}$ by circulating water with a constant temperature within the device. For each experiment, 32 frames of scattering profiles of 256 points were

sequentially stored in the process memory of the multichannel analyzer in the following time pattern: 10 frames of 60 s accumulation with a time gap of 1 s; 6 frames of 60 s accumulation with a time gap of 10 s; 5 frames of 60 s accumulation with a time gap of 60 s; 5 frames of 60 s accumulation with a time gap of 120 s; and 6 frames of 60 s accumulation with a time gap of 240 s. Ten cycles of these measurements were summed and saved on the floppy disk of a microcomputer.

Data Reduction. The scattering intensities recorded on both sides of the primary beam were averaged at equivalent points after subtracting background intensities. The center of the primary beam (zero-angle scattering) was precisely searched so as to realize the best coincidence of the scattering intensities at the equivalent points on both sides of the zero-angle. The coincidences expressed by a reliability factor $R_{\text{sym}}^{10)}$ were all good. The scattering intensity $I(s)$ was then obtained by a deconvolution (desmearing) for the beam-height effects according to the method of O. Glatter.¹¹⁾ The scattering parameter s is defined by $s = 4\pi \sin \theta / \lambda$, where 2θ is the scattering angle and λ the wavelength ($\lambda = 1.5418 \text{ \AA}$).

Results

Radius of Gyration and Zero-Angle Scattering Intensity. The radius of gyration R_g and zero-angle scat-

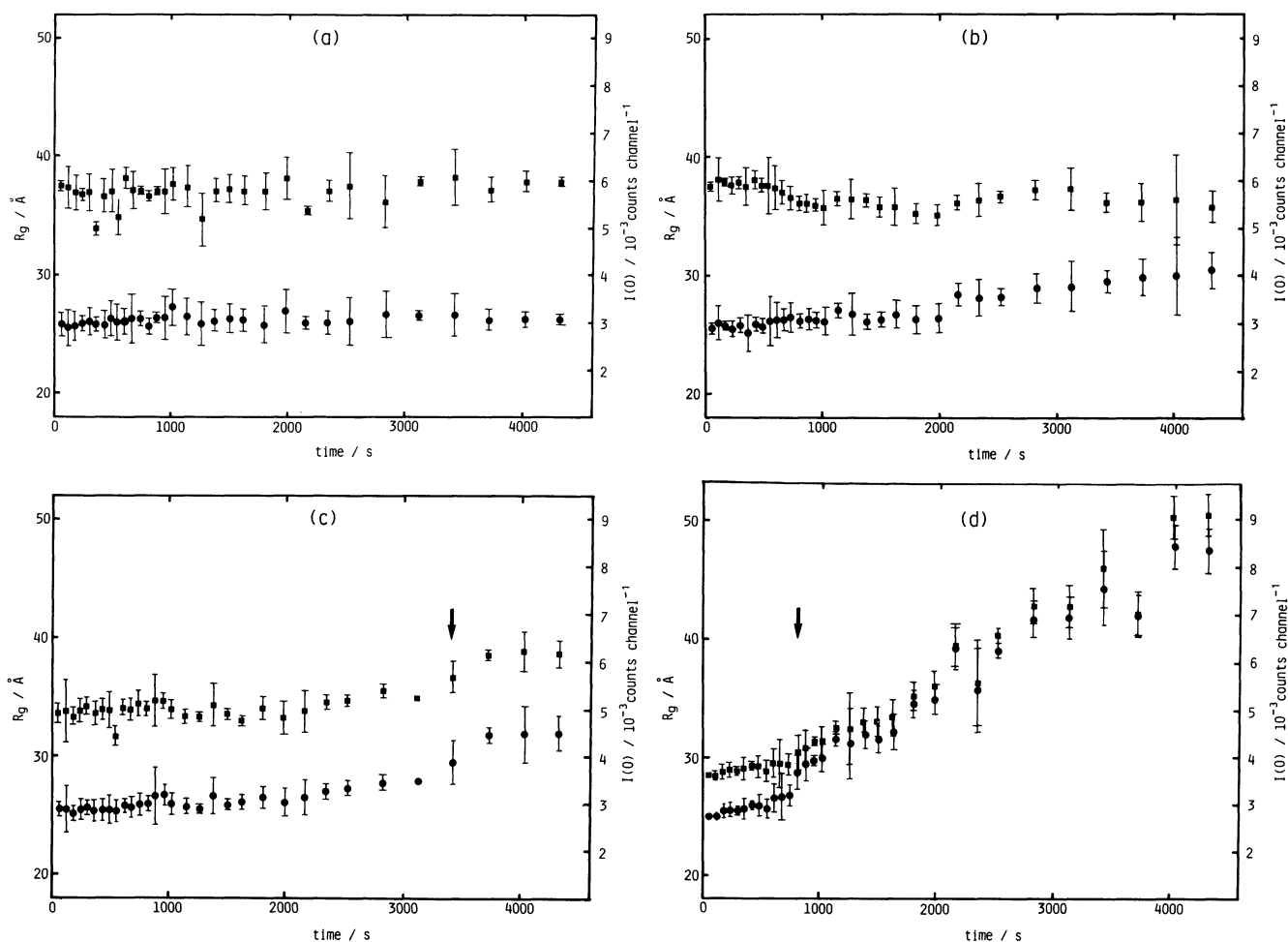


Fig. 1. Time courses of radius of gyration, R_g (●) and zero-angle scattering intensity, $I(0)$ (■): (a) at 0°C, (b) at 5°C, (c) at 10°C, and (d) at 15°C. Error bar is drawn by 3σ , where σ is the standard deviation obtained from the least-squares method.

tering intensity $I(0)$ were derived from a Guinier plot¹²⁾ of the small-angle scattering profile by a least-squares method. The time courses of R_g and $I(0)$ at each temperature are plotted in Fig. 1. At 15 °C, R_g and $I(0)$ increase appreciably after about 800 s, within the time during which R_g gradually increases and $I(0)$ remains unchanged. This phenomenon was also observed at 10 °C; however the time at which the large increases of R_g and $I(0)$ were observed was retarded to about 3400 s. At 5 °C, only the phenomenon of a gradual increase of R_g and an almost constant $I(0)$ was observed over the whole range of the time course. However, neither R_g nor $I(0)$ changed at 0 °C. These results show that the acid-denaturation of Taka-amylase A can be explained by two steps of a structural change from the time courses of R_g and $I(0)$. Also, its rate is strongly dependent on the temperature. The arrow in Fig. 1 shows the time between the first and second steps. A further analysis regarding the respective steps resulted in the following two paragraphs.

The Time Courses of Structural Parameters in the First Step. The X-ray crystal structure analysis has clarified that the Taka-amylase A molecule is an ellipsoid with approximate dimensions of $35 \times 45 \times 80$ Å.¹³⁾ Since the ellipsoid was considered to be a prolate ellipsoid of revolution with a semi-axis length of $a=20$ Å and an eccentricity of $w=2.0$, the observed scattering profile for each frame was compared with the theoretical scattering function of a prolate ellipsoid (Fig. 2). This comparison was performed in a time range in which $I(0)$ was nearly constant, because the increase of $I(0)$ corresponds to that of the molecular mass.¹²⁾ The time courses of the semi-axis lengths, a and b ($b=a \times w$), of the ellipsoid are plotted in Fig. 3. The structural parameters of the initial and the final stages in the first step are summarized in Table 1. Taking account of the hydration in solution and/or the experimental errors, the structural parameters (a , b and R_g) of the initial stage were all in good agreement with those obtained from the X-ray crystal structure analysis¹³⁾ ($a=20$ Å, $b=40$ Å) and from the ellipsoidal model with $a=20$ Å and $b=40$ Å ($R_g=22$ Å), respectively. These parameters changed with time. As shown in Fig. 3, the eccentricity w of the ellipsoid increased from 2.0 to 2.4 and the semi-axis length a did not change. However, neither a nor w changed at 0 °C. These findings indicate that the native Taka-amylase A elongates with time during the first step of the acid-denaturation.

The Time Courses of Structural Parameters in the Second Step. As described above, the increase of $I(0)$ may be attributed to an aggregation of a Taka-amylase A molecule. Figure 4 depicts Guinier plots of the small-angle scattering profiles at 15 °C. Time frames of 1, 18, 24, and 29 are plotted. The single straight line just after mixing (Fig. 4(1)) can be approximated by two lines (Fig. 4(2)–(4)) with time. The slope of the Guinier plots in the smaller-angle

region gradually increases, whereas that in the larger-angle region remains unchanged. This behavior (of the Guinier plot) suggests that the X-ray scatterer in solution is composed of two kinds of particles with different sizes.¹⁴⁾

Jellinek and Fankuchen have proven that in a poly-dispersed solution, R_g of each X-ray scatterer can be estimated from the small-angle scattering profile.¹⁵⁾ Figure 5 shows the R_g 's of the two X-ray scatterers derived from the method of Jellinek and Fankuchen using scattering profiles at 15 °C. From the figure it was found that the R_g of the large X-ray scatterer increased with time, and that of the small one remained unchanged and corresponded to that of a Taka-amylase A monomer. This is because the R_g of the ellipsoidal model of Taka-amylase A was estimated to be 27 Å.

The distance distribution function $P(r)$ ¹⁶⁾ was also calculated by a Fourier transform of the scattering profile at 15 °C. The maximal dimension D_{\max} of the particle, which was approximated at an r where $P(r)$ decreases to zero, corresponds to that of the larger particle of the two X-ray scatterers in the present system. The D_{\max} becomes larger with time as the R_g of the large X-ray scatterer.

Discussion

As shown in Fig. 1, the time courses of R_g and $I(0)$ could be described by two steps: one a gradual increase in R_g and almost constant $I(0)$, and the other a large increases in both R_g and $I(0)$. Since $I(0)$ corresponds to the square of the number of excess electrons in the X-ray scatterer (for details regarding $I(0)$, see the next stage), the nearly constant $I(0)$ throughout the time means that the morphological change (such as the aggregation or dissociation of X-ray scatterer) was not brought about by acid-denaturation. Therefore, the gradual increase in R_g implies that the internal structure of the X-ray scatterer changes without aggregation or dissociation. On the other hand, the large increase in $I(0)$ indicates that X-ray scatterers aggregate with each other through acid-denaturation; this simultaneously causes a large increase in R_g . In addition, the higher the temperature, the faster they aggregate. The details of the structural changes in the two steps are discussed in the following paragraphs, respectively.

Structural Change in the First Step. The small-angle X-ray scattering method does not give as many structural parameters as does an analysis in the crystalline state. This indicates that a unique structural model could not be constructed in some cases in spite of the recent development of such analytical method as the contrast variation.^{16,17)} Therefore, the structural change was analyzed regarding the shape of a native Taka-amylase A molecule as a prolate ellipsoid. It was ascertained by X-ray crystal structure analysis. This analysis is supported by the fact that the values of the

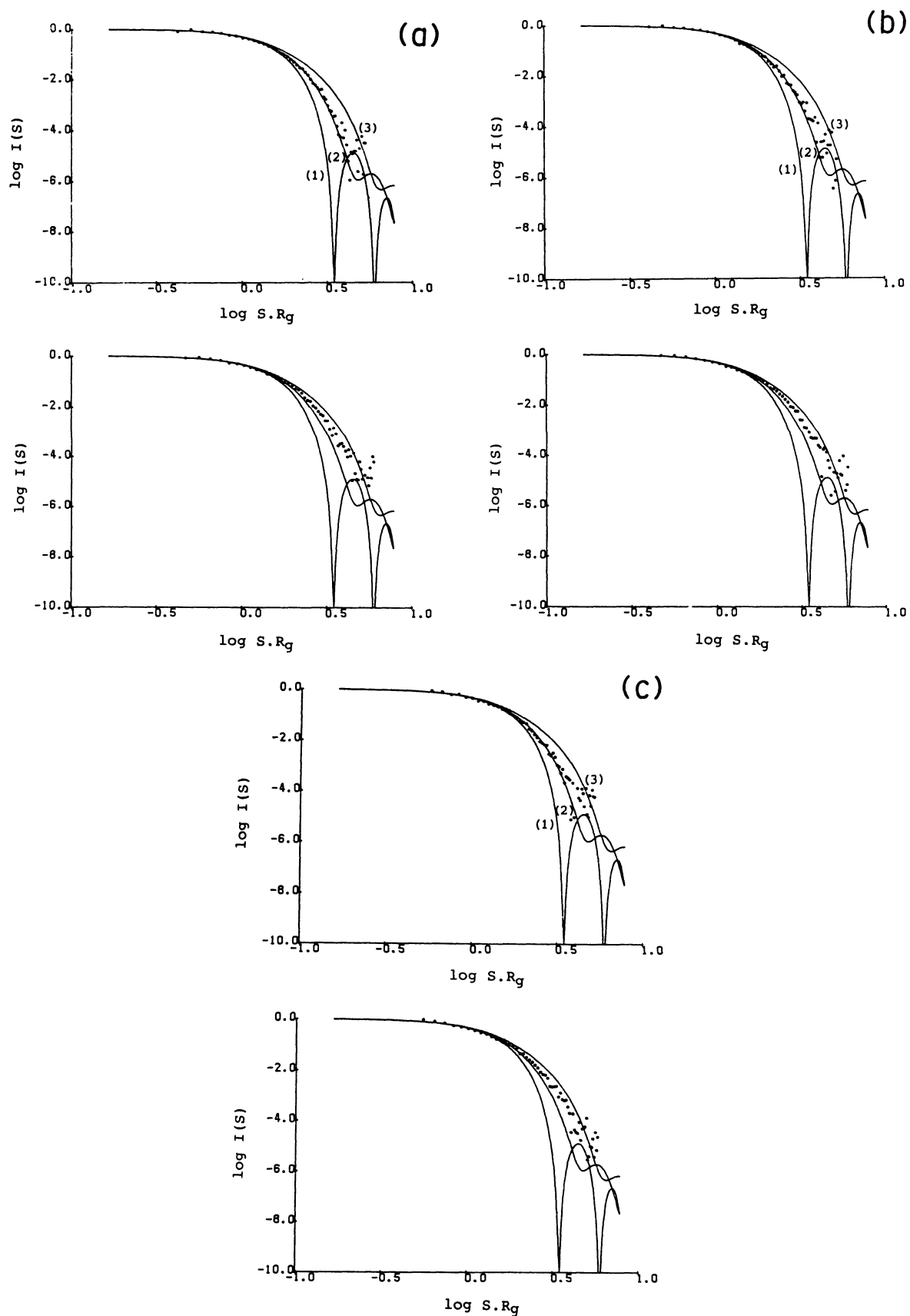


Fig. 2. $\log I(s)$ - $\log s$ plot of the observed scattering intensities (●). (a), (b), and (c) are the plots at 5, 10, and 15°C, respectively. In (a), (b), and (c), top corresponds to the time frame 1 at each temperature and bottom corresponds to the time frame 32 at 5°C, 29 at 10°C and 13 at 15°C. Superimposed are the theoretical scattering functions (solid lines) of the prolate ellipsoids with the eccentricities, w of (1) $w=1.0$, (2) $w=2.0$ and (3) $w=3.0$.

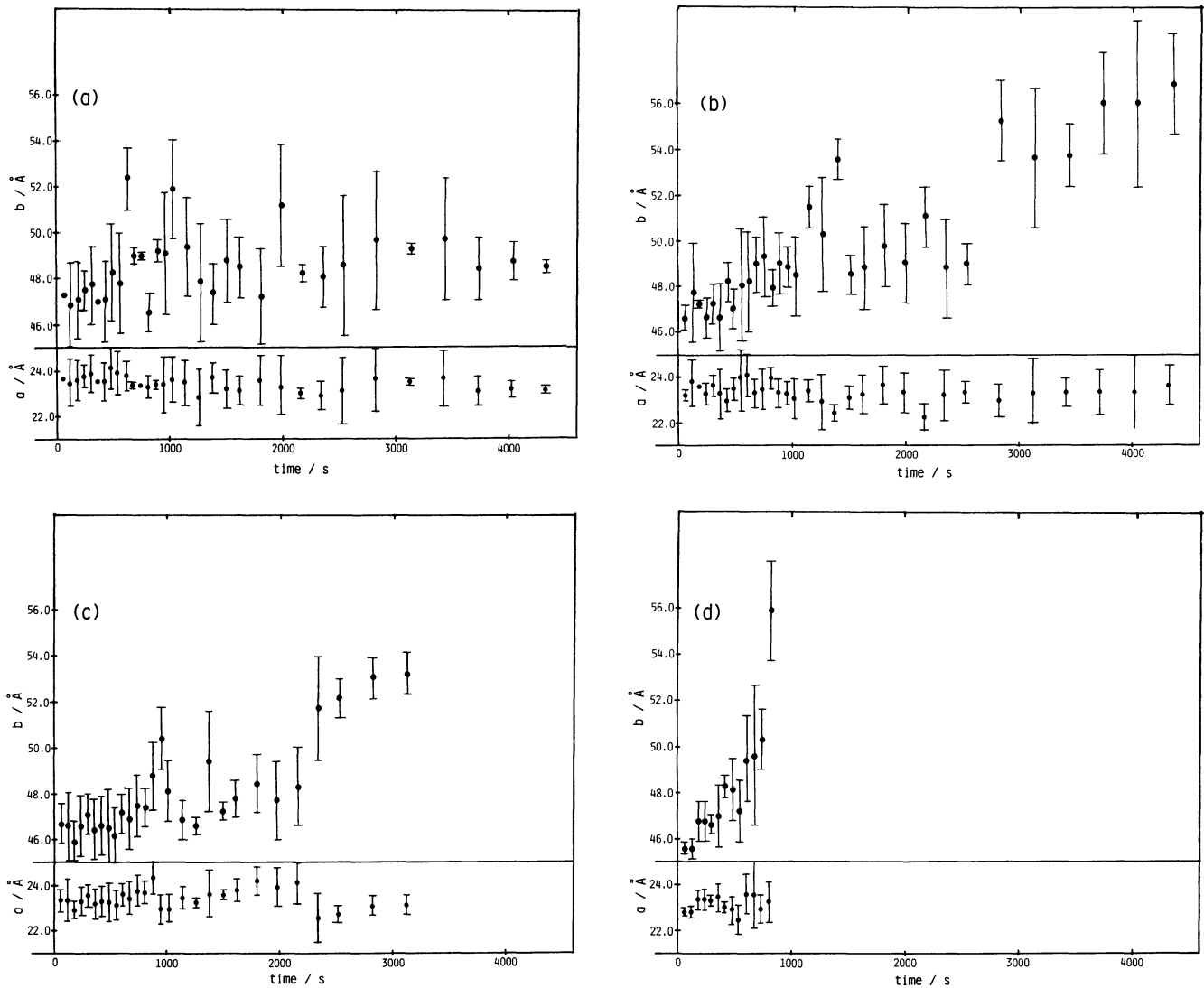


Fig. 3. Time courses of semi-axis lengths, a and b ($b=a\times w$) of a prolate ellipsoid. (a) at 0°C , (b) at 5°C , (c) at 10°C , (d) at 15°C . Error bar is drawn by 3σ , where the σ is the standard deviation obtained from the least-squares method.

Table 1. The Structural Parameters of the Initial Stage (Time 1) and the Final Stage (Time 2) in the First Step

$t/^{\circ}\text{C}$	Time 1/s			Time 2/s		
	$R_g/\text{\AA}$	$a/\text{\AA}$	$b/\text{\AA}$	$R_g/\text{\AA}$	$a/\text{\AA}$	$b/\text{\AA}$
0	60			4320		
	25.9	23.7	47.3	26.2	23.1	48.5
5	60			4320		
	25.5	23.3	46.6	30.2	23.7	56.8
10	60			3420		
	25.6	23.4	46.7	29.6	23.3	53.7
15	60			810		
	25.0	22.8	45.6	29.0	23.3	55.9

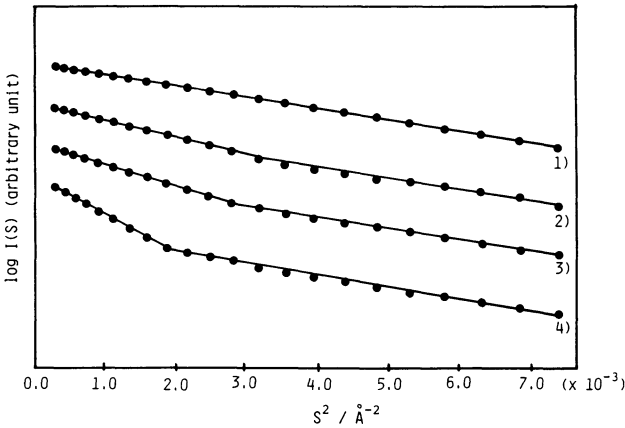


Fig. 4. Guinier plots of the small-angle scattering profiles at 15°C . Time frames 1 (1), 18 (2), 24 (3), and 29 (4) are plotted.

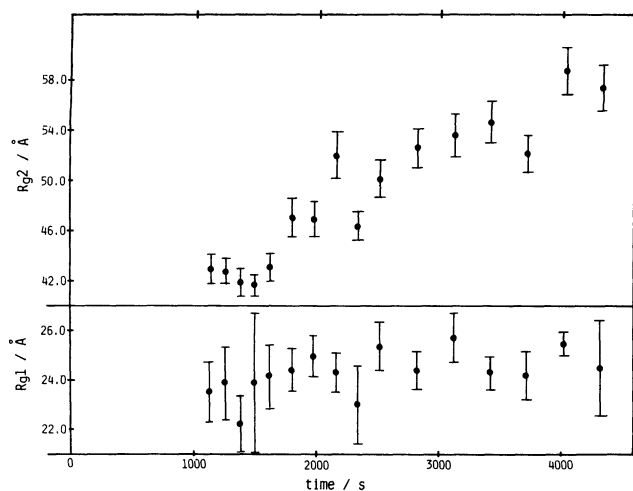


Fig. 5. Time courses of radii of gyration of a small X-ray scatterer, R_{g1} and a large X-ray scatterer, R_{g2} at 15°C. Error bar is drawn by 3σ , where σ is the standard deviation obtained from the least-squares method.

radius of gyration and the semi-axis lengths (a and b) of the ellipsoid just after mixing ($Time1$ in Table 1.) are all in good agreement with those from the X-ray crystal structure analysis. As can be seen in Fig. 3, the eccentricity of native Taka-amylase A gradually increases to about 2.4 until 800 s at 15°C, 3400 s at 10°C and 4300 s or more at 5°C. The semi-axis length a was constant throughout all time. These results show that a Taka-amylase A molecule extends along the b -axis. However, since this extension of the molecule reduces the difference between the average electron densities of the molecule and the solvent, $I(0)$ must gradually decrease, because $I(0)$ is directly proportional to the square of the number of excess electrons in the molecule (sum of the electron density difference over the molecule). The actual state in which $I(0)$ is almost constant may arise from an experimental error in $I(0)$.

Takagi and Toda⁶⁾ have indicated that by acid-denaturation the hydrogen bonds between side-chain groups were completely cleaved and most of the peptide hydrogen bonds were retained to maintain a helical region; that is, most helical structures of a Taka-amylase A molecule remain during acid-denaturation. The fact that the eccentricity of the prolate ellipsoid gradually increases and the semi-axis length a is unchanged may arise from a cleavage of the hydrogen bonds between the side-chain groups. This is because a complete destruction of secondary and tertiary structures is expected to provide more drastic changes in the structural parameters. The CD spectra of acid-denaturated Taka-amylase A also showed little difference regarding the α -helix content between native Taka-amylase A and the acid-denaturated one.

The X-ray crystal structure analysis³⁾ has also clarified the fact that native Taka-amylase A is composed of

two large domains (main domain and C-terminal domain) with a narrow cleft between them. These domains are linked by a single polypeptide chain and stabilize each other with some hydrogen bonds. Therefore, the cleavage of the hydrogen bonds by acid-denaturation is expected to cause an increase in the molecular eccentricity; this is because a domain is supposed to be the folding unit of a protein¹⁸⁾ and most of the hydrogen bonds are more stable than those between the two domains. A $(\beta\alpha)_8$ super-secondary structure (β -barrel), similar to those of triose phosphate isomerase,¹⁹⁾ pyruvate kinase²⁰⁾ or aldolase²¹⁾ is found in the main domain of the native Taka-amylase A. The β -barrel contains the active site and protects against the destruction of the large cleft located in the main domain. The destruction of the cleft by the cleavage of the hydrogen bonds is also considered to be one of the factors which cause an elongation in the native molecule.

The small-angle X-ray scattering method, however, does not give much information concerning the internal structure of a molecule. As a result, no direct experimental evidence for the cleavage of the hydrogen bonds between the domains and the destruction of the β -barrel structure has been obtained in the present analysis. It is necessary to analyze the middle- and high-angle scattering intensities which give information about the internal structure. The correlation of the middle- and high-angle scattering intensities with secondary and tertiary structures of protein is now being investigated in our laboratory.

Structural Change in the Second Step. As shown in Fig. 4, the Guinier plot of the small-angle scattering profile at 15°C became biphasic with time. This phenomenon indicates that the X-ray scatterer in a solution comprises two kinds of particles with different sizes. Using analyses by the method of Jellinek and Fankuchen as well as the distance distribution function, it was elucidated that the large particle further expanded with time and the small one remained unchanged. The R_g of the small particle showed a good coincidence with that of Taka-amylase A monomer. These results indicate that Taka-amylase A molecules aggregate with each other and the X-ray scatterer in solution consists of a large aggregate and a small elongated molecule transformed from native Taka-amylase A by a partial unfolding of the polypeptide chain.

It was, however, shown from a sedimentation velocity study that acid-denaturated Taka-amylase A molecules became highly aggregated with each other to different degrees.⁶⁾ However, this may result from the differences in the times at which the X-ray scattering intensities and the sedimentation patterns of Taka-amylase A were measured. In the present X-ray analysis, Taka-amylase A molecules started to aggregate with each other at 800 s after the molecules began to be denaturalized at 15°C. However, in the sedimentation

velocity study, the sedimentation patterns were measured in an acid-denaturated Taka-amylase A solution dialyzed against a 0.02-M glycine-HCl buffer (pH 2.2) for one day after the enzyme solution was acidified to pH 2.2.⁶⁾

We thank Professor Masao Kakudo for his interest, valuable discussions, and warm encouragement throughout this study.

References

- 1) S. Akabori and K. Okahara, *Bull. Chem. Soc. Jpn.*, **12**, 55 (1937).
 - 2) H. Toda, K. Kondo, and K. Narita, *Proc. Jpn. Acad.*, **58B**, 202 (1982).
 - 3) Y. Matsuura, M. Kusunoki, W. Harada, N. Tanaka, Y. Iga, N. Yasuoka, H. Toda, K. Narita, and M. Kakudo, *J. Biochem.*, **87**, 1555 (1980).
 - 4) Y. Matsuura, M. Kusunoki, W. Harada, and M. Kakudo, *J. Biochem.*, **95**, 697 (1984).
 - 5) T. Takagi and T. Isemura, *J. Biochem.*, **49**, 43 (1961).
 - 6) T. Takagi and H. Toda, *J. Biochem.*, **52**, 16 (1962).
 - 7) T. Takagi and T. Isemura, *J. Biochem.*, **52**, 314 (1962).
 - 8) S. Akabori, T. Ikenaka, and B. Hagihara, *J. Biochem.*, **41**, 577 (1954).
 - 9) A. Franks, *Proc. Phys. Soc. London, Sect. B.*, **68**, 1054 (1955).
 - 10) T. L. Blundel and L. N. Johnson, "Protein Crystallography," Academic Press, London (1976), pp. 318—319.
 - 11) O. Glatter, *J. Appl. Crystallogr.*, **7**, 147 (1974).
 - 12) A. Guinier and G. Fournet, "Small Angle Scattering of X-Rays," John Wiley and Sons Ltd., New York (1955), pp. 24—28.
 - 13) Y. Matsuura, M. Kusunoki, W. Date, S. Harada, S. Bando, N. Tanaka, and M. Kakudo, *J. Biochem.*, **86**, 1773 (1979).
 - 14) A. Guinier, "Theorie et Technique de la Radio-cristallographie," Dunod, Paris (1964).
 - 15) M. H. Jellinek and I. Fankuchen, *Ind. Eng. Chem.*, **37**, 158 (1945).
 - 16) O. Glatter and O. Kratky, "Small Angle X-ray Scattering," Academic Press, New York (1982), pp. 130—131.
 - 17) H. B. Stuhmann and A. Miller, *J. Appl. Crystallogr.*, **11**, 325 (1978).
 - 18) G. E. Schulz and R. H. Schirmer, "Principles of Protein Structure," Springer-Verlag, New York (1978), Chap. 5.
 - 19) D. W. Banner, A. C. Bloomer, G. A. Petsko, D. C. Phillip, C. I. Pogson, and I. A. Wilson, *Nature*, **255**, 609 (1975).
 - 20) D. I. Stuart, M. Levine, H. Muirhead, and D. K. Stammers, *J. Mol. Biol.*, **134**, 109 (1979).
 - 21) J. S. Richardson, *Biochem. Biophys. Res. Commun.*, **90**, 285 (1979).
-